WARSAW UNIVERSITY OF TECHNOLOGY Index 351733
FACULTY OF CIVIL ENGINEERING
COMMITTEE FOR CIVIL AND WATER ENGINEERING
POLISH ACADEMY OF SCIENCES ISSN 1230-2945

DOI: 10.24425/ace.2025.153352

ARCHIVES OF CIVIL ENGINEERING

Vol. LXXI ISSUE 1 2025

pp. 595–613

Research paper

The method of predicting tightening torque and preload for bolts embedded in softwood using steel washers

Bartosz Kawecki[1]

Abstract: The paper presents an investigation on tightening torque and preload prediction for bolts embedded in softwood using steel washers. A basis for the research was a lack of any information on the tightening torque value for bolted connections in the timber structures' design codes. For this reason, two experimental tests, theoretical analysis and Finite Element modelling, were performed in the paper. The first experiment based on finding the tightening torque to relative displacement relationship. The next one enabled the author to check the maximal compressing force determined by theoretical approach. In this test, dependencies between plastic modulus including material's compaction and modulus of elasticity were found too and then applied to the numerical model. Tightening torque was calculated according to agreed formulas elaborated for steel structures based on the obtained preload force value. The high correlation between results from the prepared numerical models and experimental tests was observed. The research presented in the paper has multiple applications, as estimating a proper tightening torque value that should clamp a bolted connection, predicting stresses in connection's components and clamping pressure when connecting several elements due to tightening torque and bolt preload force introduction or predicting the structural response of multiple bolts connections in the first phase of the loading.

Keywords: preload and tightening torque prediction, bolts embedded in softwood, experimental tests, Finite Element modelling

[1]PhD., Eng., Lublin University of Technology, Faculty of Civil Engineering and Architecture, ul. Nadbystrzycka 40, 20-618 Lublin, Poland, e-mail: b.kawecki@pollub.pl, ORCID: 0000-0001-8134-5956

1. Introduction

Connections in wooden structures can be done with many methods. These done with mechanical fasteners, as dowels, screws, or bolts are still popular. The frequently observed phenomenon is an indentation near a fastener, both during structure exploitation or assembly. The construction work phase, understood as a wood indentation in parallel to grain direction, is well-described and examined in the literature [1–7]. However, an indentation can be observed in the mounting phase too due to low wood strength in perpendicular to grain direction. This issue is especially important in bolted connections, where an applied force can be significant comparing to wood properties. Pretension usually remains not high enough to exceed a load-carrying capacity of the bolt, but material's damage in places where the pressure from bolt head, nut, or steel washer is applied may occur and affect a connection's mechanical performance. This commonly happens in typical elements' connecting directions, as radial or transversal, being simultaneously followed by the weakest wood material properties. A tightening torque value of bolts embedded in wood is not defined anywhere in the series of European Codes EN-1995 [8] on the timber structures' design. The only rule says that elements should be assembled firmly. On a lack of thorough investigations in the field, the topic being examined includes bolt pretension and tightening torque estimation.

The first part is compound of experimental tests on tightening torque and pretension load in wooden members. Siqueira and Menezzi [9] tested an effect of the torque on the ultimate load of structural fastenings for wood bolted joint. Hexagonal bolts were utilised to evaluate the maximal load according to five torque levels for two wood sections in compression parallel to the wood grain. The ultimate load amplified until a specific torque level, guiding the authors to the statement that a control of the torque of the bolted joint can be significant. Awaludin et al. [10] examined the effect of preload in bolts on damping response and ultimate moment-carrying capacity of timber joint with steel side plates. The pre-stressed joint's superiority was showed by a significant increase in initial stiffness and a small increase in ductility and ultimate moment resistance. The preload force was stated to increase the structural performance of timber joints that carried moments. Next, in [11] the authors stated that introducing preload force into the bolts can increase the connection's stiffness at the initial loading phase by causing higher friction between the adjacent elements. The failure forms of joints were similar regardless of applied preload value. They analysed several samples with varying pretension forces and results proved that the higher the pretension force, the higher ultimate lateral load is. Subsequently, in [12] the effectiveness of bolts pretension after one year of stress relaxation measurement was evaluated. Nine pre-stressed joints were prepared and exposed to indoor conditions. Several specimens were re-stressed after three and six months with a regular measurement of relaxation. Then, the joints were loaded in cycles and monotonically up to failure. The initial pre-stressing effect was negligible without regular re-stressing. Their last work [13] included large displacements cyclic tests, where beam to column timber joints with steel side plated were tested up to damage. The results, got for four different pretension magnitudes, showed that the bolts preload supersize the frictional damping, but had no significant influence on the ultimate connection' resistance. Vieira et al. [14] aimed to evaluate the effect of the torque value over time. An assembly was done using four hexagonal

bolts with washers and nuts using two torque levels. Then, the samples were split into two groups, with one group tested immediately and the other group tested six months later. The results showed that torque improved the properties of the samples tested just after assembling, but after six months, the positive effect was lost. Matsubara et al. [15] tried to find empirically how the torque influences the separation in bolted joints loaded axially. The ultimate tensile load was stated to decrease when the preload force increased.

The second part provides a preface to torque-preload calculations. Izumi et al. [16] investigated the loosening of the tighten connections in shear loading by a 3D finite element model. Results were compared with theoretical approaches and experimental data. The preload to tightening torque relationship was stated to show a good agreement between the FE model and the theoretical approach. Yu et al. [17] established a detailed 3D finite element model of bolted joints, considering such details as helix angle, pitch, thread or tooth angle. The results showed that the friction coefficient between nut and the joint has a dominant influence on the relationship between torque and preload. In the next work [18] authors studied the torque-preload relationship by using their own torque-only control method. Gong et al. [19] used a 3D finite element model to get the actual bearing pressure distribution, and thus the effective bearing contact radius. Subsequently, the effects of geometrical, material and frictional factors were explored. Noteworthy is the fact that the analytical models for calculating torque-preload relationship are developed for steel structures, where small displacements occur due to a high material's stiffness. Wooden structures are characterised by a low modulus of elasticity perpendicular to grains, being 700 times lower and yielding stress being 100 times lower than for steel material. The homogeneity of the material is also significantly lower in natural materials. The tightening-torque relation is up to now unrecognised and not modelled. This requires a thorough analysis with assumptions different from steel structures.

2. Materials and methods

The entire idea of the article was to check a behaviour of a single bolt being embedded in a cuboid wooden sample using steel washers under preloading application. These studies were conducted to discuss gaps in the existing literature. The aim was to estimate tightening torque value and preload force utilising small scale experimental tests supported by computer modelling with the Finite Element Method (FEM). Experimental and computational testing programme was performed with fully threaded M6 5.8 class bolts being embedded in spruce wood of moisture content between 10–13% and density between 420–480 kg/m^3 using steel washers with three different diameters.

2.1. Experimental assumptions and theoretical relations

Firstly, an experimental measurement of tightening torque relating to a relative displacement $T_f(2 \cdot \delta_t)$ was performed. Nuts were tightened using certified Wera dynamometric screwdrivers with the range of 0.3–6.0 N · m. Tightening torque resolution depended on a screwdriver – 0.05 N·m, 0.1 N·m and 0.25 N·m for 0.3–1.2 N·m, 1.2–3.0 N·m, and 3.0–6.0 N·m, respectively.

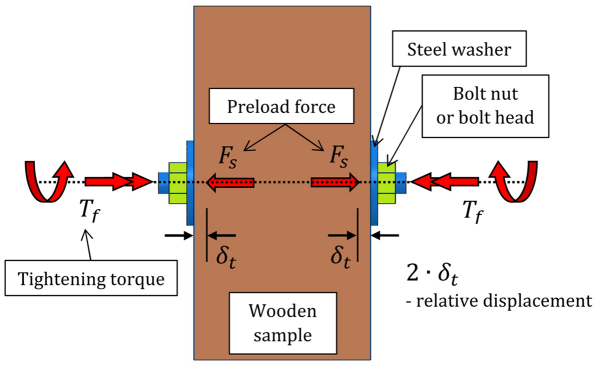

Fig. 1. Graphical description of the tightening torque to relative displacement measurement

Relative displacement measurements were done with Hogetex electronic micrometer with precision 0.001 mm. The graphical description of the measuring manner was presented in Fig. 1.

Six samples per each steel washer's diameter were prepared to obtain a statistically valid number of measurements. An initial tightening torque equal to 0.5 N · m was used to set the bolt in a wooden sample using self-locking nuts just to remove clearance. The value was empirically tested by screwing several self-locking nuts on several bolts. The exemplary specimens, one per each steel washer's diameter were presented in Fig. 2.

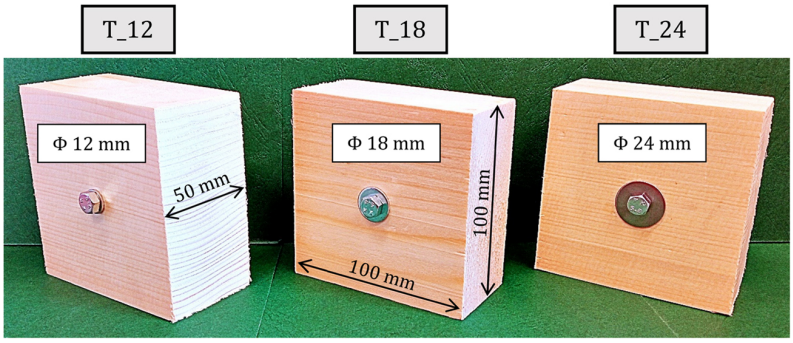

Fig. 2. Exemplary specimens for each steel washer's diameter

The experimental procedure was measuring the initial length between the bolt head and nut, then tightening the nut with a known torque value set on a dynamometric screwdriver with measuring the changed length. The number of screwing times was based on Yu work [18], who found that at least three times screwing of the nut is required to set a stable torque value. Subtraction of the measured value from the initial one was a relative displacement ($2 \cdot \delta_t$). Next, the step was subsequently repeated, which resulted in obtaining torque to relative displacement relationship for each tested sample. Tests were carried out up to reaching 1.5 mm displacement or 5.5 N · m torque value.

With bolts being embedded in wood using steel washers, a load-carrying area is small, which causes a necessity to treat compressing load as a point concentrated force. In this scenario, the vicinity of the load can be treated as isotropic, with properties dependent solely on perpendicular-to-grain properties. The mean material properties of spruce wood needed in the model as modulus of elasticity, Poisson ratio and strength perpendicular to grains, were calculated based on Wood Handbook [20] and were equal to $E_{c.90} = 0.3$ GPa, $\nu = 0.45$ and $f_{c.90} = 3.5$ MPa, consecutively.

With this assumption, the maximal compressing force in elastic range ($F_{c.90}$) can be predicted based on formulas by Leijten et al. [21, 22] and Van der Put [23] (2.1):

$$F_s = F_{c.90} = f_{c.90} \cdot k_{c.90} \cdot A_c, \qquad k_{c.90} = \sqrt{\frac{d_{ef}}{d_w}}$$
$$A_c = \frac{\pi}{4}\left[\left(d_w + \frac{h_e}{3}\right)^2 - d^2\right], \qquad h_e = 0.4 \cdot \frac{t}{2}, \qquad d_{ef} = d_w + \frac{h_e}{3} \tag{2.1}$$

where: $f_{c.90}$ – wood strength perpendicular to grain, $k_{c.90}$ – coefficient of stress dispersion, A_c – effective load-carrying area, d_{ef} – effective load-carrying diameter, d_w – diameter of steel washer, h_e – indentation depth, d – diameter of an opening in wood, t – thickness of a wooden specimen.

The wood compliance can be approximated according to averaged load-carrying area based on real steel washer's diameter (d_w) and the effective one (d_{ef}). The indentation depth defined as (h_e) leads to mean volume determination, which can be used as a hollow cylinder simplification in a numerical model. The assumption was presented in Fig. 3.

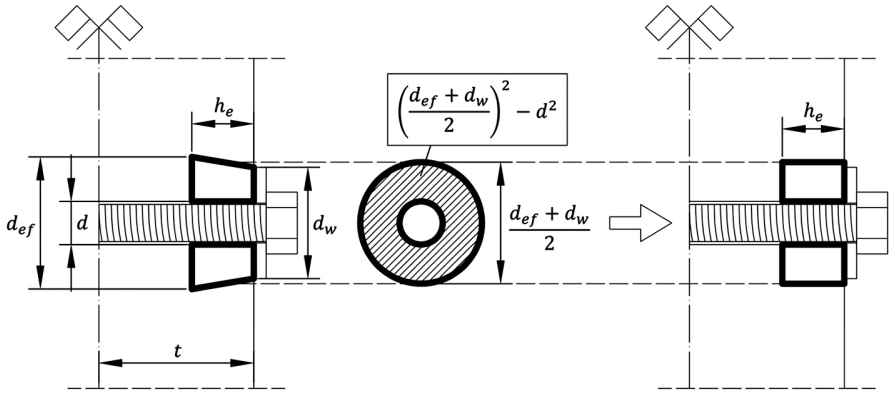

Fig. 3. The description of a hollow cylinder simplification for numerical model

Total compliance of the setup can be determined as a sum of bolt and wood compliance. Both can be determined as follows (2.2):

$$\frac{1}{s} = \frac{1}{s_b} + 2\frac{1}{s_w}, \qquad \frac{1}{s_b} = \frac{4 \cdot L_b}{\pi \cdot E \cdot d_p^2}, \qquad \frac{1}{s_w} = \frac{4 \cdot h_e}{\pi \cdot E_{c.90} \cdot \left[\left(\frac{d_{ef}+d_w}{2}\right)^2 - d^2\right]} \tag{2.2}$$

where: s_w – wood stiffness, s_b – bolt stiffness, E – modulus of elasticity of steel, d_p – effective diameter of the bolt's thread, L_b – length of the bolt.

Applying the mean value of modulus of elasticity perpendicular to grains makes possible to calculate mean relative displacement at the level of maximal linear preloading force, as follows (2.3):

$$2 \cdot \delta_t = \frac{F_s}{s} \tag{2.3}$$

The known value of the mean relative displacement provides a possibility of comparing the preloading force (F_s) to the tightening torque (T_f). Because the maximal compressing force ($F_{c.90}$) was elaborated with theories available in the literature, the need for experimental check appeared. To examine the issue, an indentation test was conducted on Zwick/Roell 2.5 kN testing machine, as presented in Fig. 4.

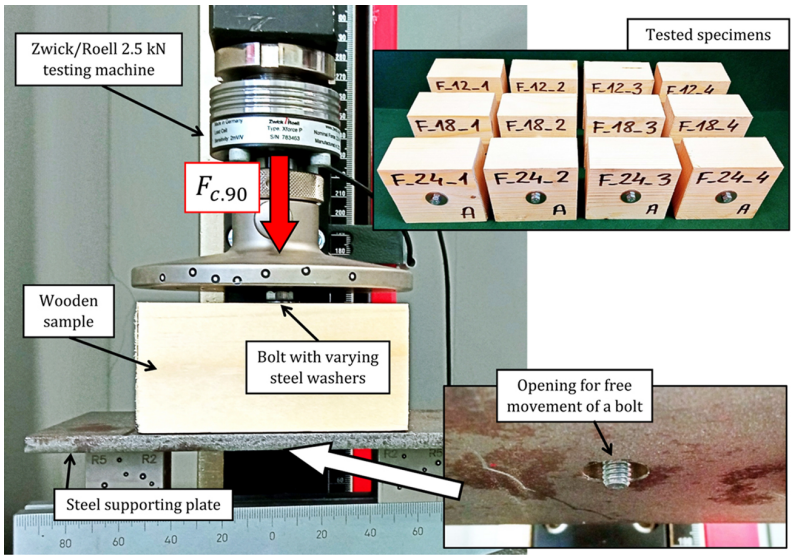

Fig. 4. Indentation test performed o Zwick/Roell 2.5 kN testing machine

Four samples per each steel washer's diameter were prepared and then tested from both sides, which resulted in eightfold force determination for each steel washer's diameter. The tested force values were compared to the theoretical ones and further discussion was done in the results and discussion section.

2.2. Numerical model assumptions

Based on the information included in the earlier section, the places of bolt's insertion can be simulated as a local hollow cylinder inclusion in a wood material with diameter equal to the one presented in Fig. 3. Then the material in this place can be modelled as isotropic with properties

according only to the perpendicular to grain properties of wood. The remaining parts of the structure can be modelled with various properties based on the predicted behaviour. This choice can be very useful because mesh in a vicinity of steel washer can be fitted, leading to correct stress distribution. Next, in a plastic stage indentation can be simulated in a further connection's work. Connection between inclusions and other part of the material can be provided by TIE constraint available in Simulia ABAQUS. The idea was presented graphically in Fig. 5.

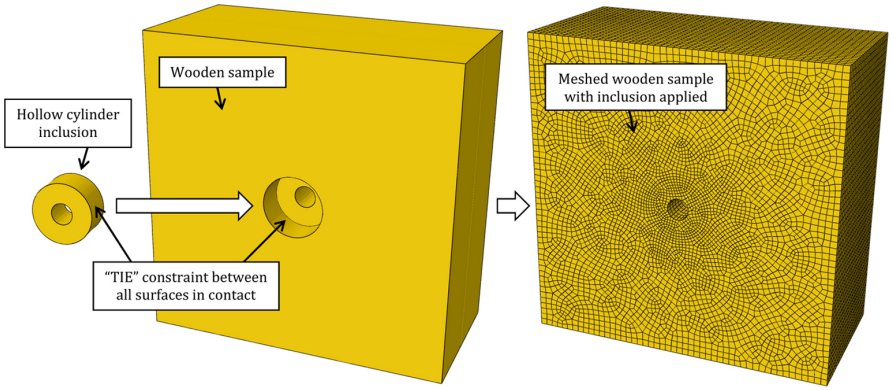

Fig. 5. Inclusions assumption for numerical modelling

Softwood material constitutive law (Figure 6a) was described by modulus of elasticity ($E_{c.90}$) and strength ($f_{c.90}$) perpendicular to wood grains, including plasticisation with compaction observed in experimental tests, resulting in the plastic modulus of elasticity being equal to ($E_{pl.90} = 0.4 \cdot E_{c.90}$).

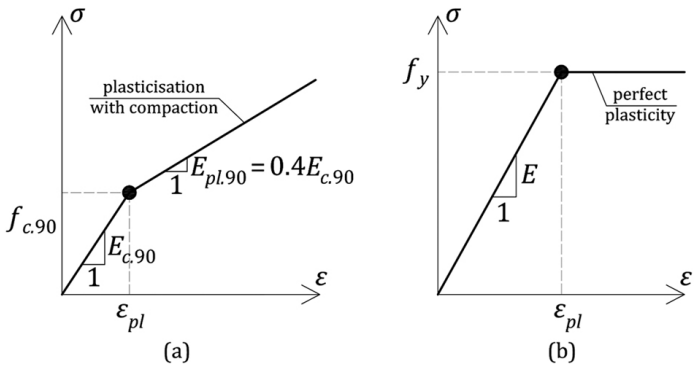

Fig. 6. Constitutive laws of the materials used in FE model: (a) Wood, (b) Steel

Steel elements' constitutive law (Figure 6b) was described by modulus of elasticity $E = 210$ GPa and perfect plasticity, but divided into two parts for plastic response – bolt M6 head and thread had 5.8 class, so the yielding stress was assumed as $f_y = 400$ MPa, while for steel washer of the thickness 1.6 mm, made of A2-304 stainless steel, this was $f_y = 190$ MPa, as

produced declared. The simplified steel material model was justified, because this was used only to find places of possible plasticisation. Finally, in the testing range, no significant exceeding of yielding strength was observed. The bolt opening had a bigger diameter (7 mm) than the bolt according to the wooden structures' codes. This caused no contact occurrence between bolt and opening surface. Zero displacements boundary conditions (UX = UY = UZ = 0) were applied to the bottom surface. According to [24] reduced integration elements in at least number of four were needed to omit hour-glassing, shear locking and other undesirable effects. C3D8R elements with dimensions of 1 mm for bolts or steel washers and 1 mm for wood in plane were used, as reasonable size to prepare proper discretisation the circular components and to provide suitable transfer of the contact between members. First, 1 mm dimension was used in normal direction, too. However, calculations lasted too long and 2 mm was used in the final version, which resulted in speeding computations at least twice with no differences in precision. The mesh quality was verified by default shape and size metrics available in Simulia ABAQUS software and no warnings were found. The checked values of the friction coefficient between components tested in the model varied between 0 and 0.5. Frictionless contact and 0.5 value resulted in problems with calculations convergence. Despite the high discrepancy in the checked friction coefficients, only slight differences in the results at the level of 1% for 0.1–0.4 values were observed. The friction coefficient causing the best stability of the model and fastest calculations was equal to 0.1 and thus this was used in further calculations. The model assumptions were presented in Fig. 7.

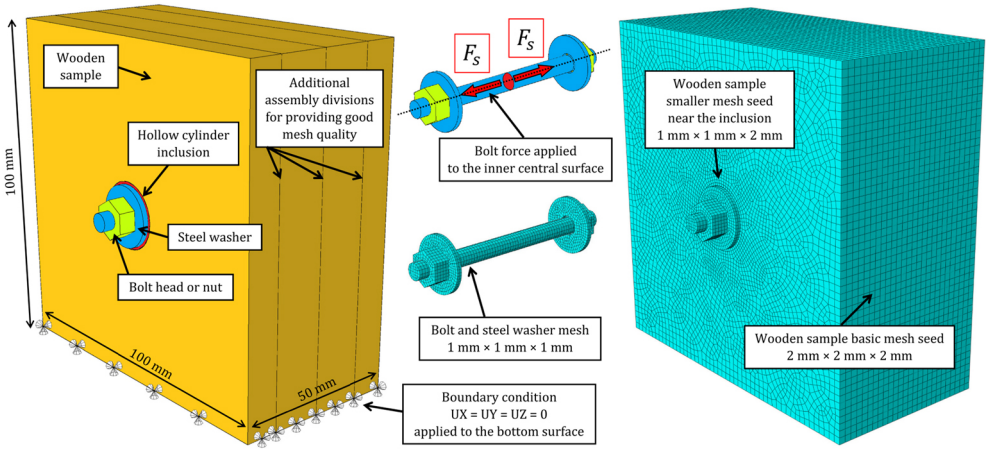

Fig. 7. FE model assumptions

Preload force (F_s) was applied to the central surface of the bolt's thread using "bolt load" available in Simulia ABAQUS software. Analyses were performed using Simulia ABAQUS/Standard solver.

3. Results and discussion

Results and discussion section were divided into two parts. The first one included experimental and theoretical relations, while the second one – numerical modelling. These two parts refer to the section materials and methods.

3.1. Experimental and theoretical relations

As several measurements of the maximal compressing force ($F_{c.90}$) were done, an uncertainty estimation was performed for experimental data. It is recommended to use the standard deviation of the mean for experimental measurements. Uncertainty can be measured by mean variance. An arithmetic mean is taken as a result of x measurement. Thus, the uncertainty of measurement is given by formula (3.1):

$$x = \overline{x} = \frac{\sum x_i}{n} \rightarrow s_{\overline{x}} = \sqrt{\frac{\sum (x_i - \overline{x})^2}{n(n-1)}} \tag{3.1}$$

where: x – measurement, $\overline{x}$ – measurement mean, n – number of measurements, $s_{\overline{x}}$ – measurement uncertainty

Table 1 presents maximal compressing force ($F_{c.90}$) measurements and simplified statistical analysis of the results depending on the steel washer's diameter.

Table 1. Maximal compressing force ($F_{c.90}$) measurements and properties for uncertainty estimation

Specimen number	**F_12 (ϕ = 12 mm)**		**F_18 (ϕ = 18 mm)**		**F_24 (ϕ = 24 mm)**	
	$F_{c.90}$ (N)	**$(x_i - \overline{x})^2$ (N^2)**	**$F_{c.90}$ (N)**	**$(x_i - \overline{x})^2$ (N^2)**	**$F_{c.90}$ (N)**	**$(x_i - \overline{x})^2$ (N^2)**
1	627.35	5403.30	1286.77	272.79	2083.87	4279.79
2	700.34	21460.96	1188.36	13207.48	1919.63	9764.60
3	455.80	9612.59	1596.23	85821.06	2144.97	16007.29
4	407.67	21366.94	1320.58	299.37	1632.23	149159.24
5	641.65	7710.93	1203.06	10043.45	1932.93	7313.59
6	682.68	16599.52	1245.86	3297.56	1934.86	6986.67
7	473.48	6458.09	1340.90	1415.01	2371.65	124755.66
8	441.77	12560.44	1244.49	3456.22	2127.43	11877.84
Satistical analysis	$\overline{x}$ (N)	Σ (N^2)	$\overline{x}$ (N)	Σ (N^2)	$\overline{x}$ (N)	Σ (N^2)
	553.84	101172.77	1303.28	117812.93	2018.45	330144.67
	$s_{\overline{x}}$ (N)	$\frac{s_{\overline{x}}}{\overline{x}}$ (%)	$s_{\overline{x}}$ (N)	$\frac{s_{\overline{x}}}{\overline{x}}$ (%)	$s_{\overline{x}}$ (N)	$\frac{s_{\overline{x}}}{\overline{x}}$ (%)
	42.50	7.67	45.87	3.52	76.78	3.80

The relative error was less than 10% for F_12 and less than 5% for F_18 and F_24 specimens. In the next step, the theoretical maximal compressing force calculated based on

formula (2.1) was compared to the values obtained in experimental tests, which were collected in Table 2. The calculated values were close enough to the mean experimental measurements. Therefore, the correctness of the adopted theoretical assumptions was proven.

Table 2. Comparison between values determined from theoretical approach and from experiments

Specimen type	$\mathbf{F_{c.90.calc}}$ **(N)**	$\mathbf{F_{c.90.mean.exp}}$ **(N)**	**Relative error (%)**
F_12	578.3	553.8	4.4
F_18	1215.3	1303.3	6.8
F_24	2048.0	2018.5	1.5

When the maximal compressing force was confirmed, the elastic compliance could be determined according to the formula (2.2) and (2.3). The calculated values were collected in Table 3.

Table 3. Values determined from theoretical approach

Specimen type	$\mathbf{F_s}$**=**$\mathbf{F_{c.90}}$ (N)	$\mathbf{2{\cdot}\delta_t}$ **(mm)**
T_12	578.3	0.362
T_18	1215.3	0.318
T_24	2048.0	0.307
Mean		**0.33**

When the elastic compliance was known, possible was to find the value of maximal elastic tightening torque value using the 2° polynomial approximations based on residual sum of squares method with coefficient of determination $R^2 > 0.9$. The found values and polynomials' formulas were presented in Fig. 8.

Next, the relationship between tightening torque and preloading force can be found (Fig. 9) and coefficient called nut factor to bolt diameter ($k_f \cdot d_b$) can be determined.

The value of nut factor to bolt diameter ($k_f \cdot d_b$) depends on several properties of the used bolts. The basic formula for assumption of uniform contact pressure and the rigid body approximation of the clamped part can be written as (3.2):

$$T_f = k_f \cdot d_b \cdot F_s, \quad k_f \cdot d_b = \frac{1}{2} \cdot \left(\frac{p}{\pi} + \frac{\mu_s \cdot d_p}{cos(\beta)} + \mu_w \cdot D_v \right), \quad D_v = \frac{2}{3} \cdot \frac{\left(d_n^3 - d_h^3\right)}{\left(d_n^2 - d_h^2\right)} \tag{3.2}$$

where: k_f – nut factor, d_b – nominal diameter of the bolt, p – pitch of thread, μ_s – friction coefficient on the thread surface, d_p – effective diameter of the thread, β – half of the thread profile angle, μ_w – friction coefficient on the nut bearing surface, D_v – equivalent diameter of friction torque on the nut-bearing surface, d_n – diameter of the nut-bearing surface, d_h – diameter of the bolt insert hole.

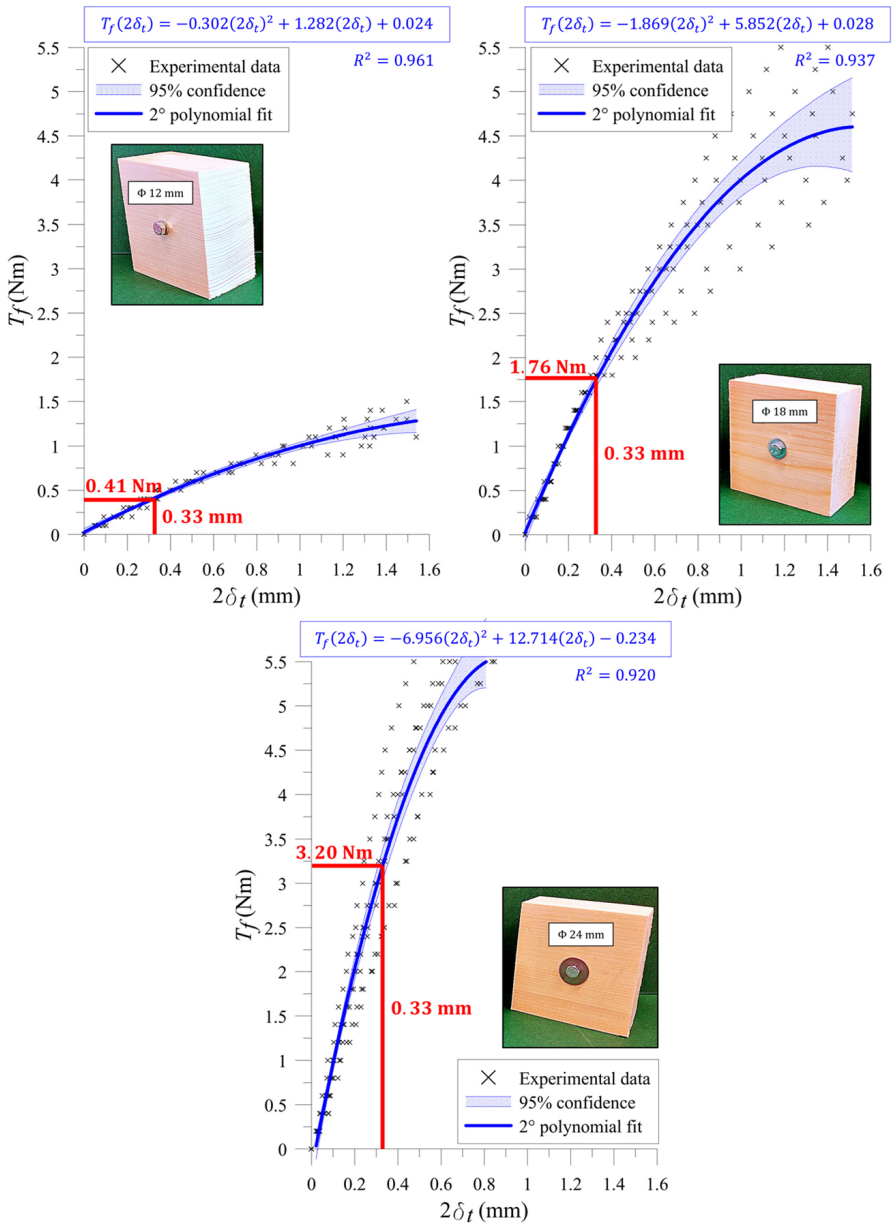

Fig. 8. Experimental tests on tightening torque to relative displacement relation

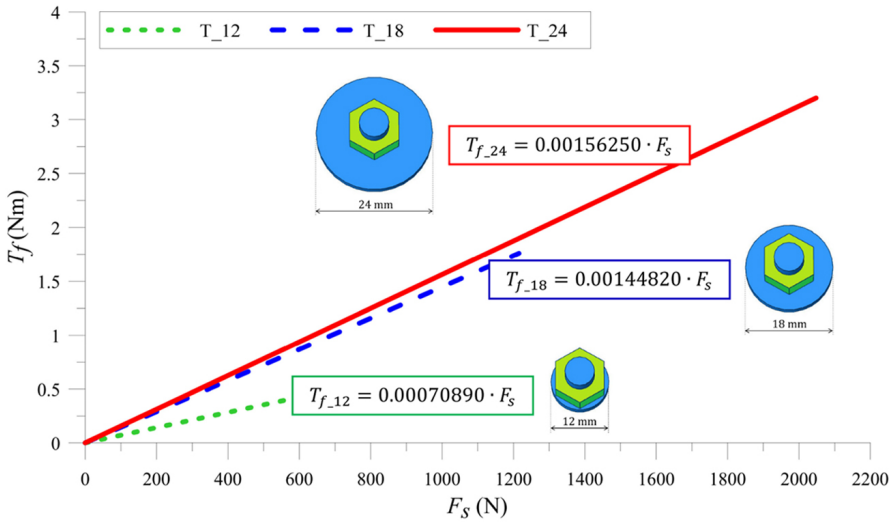

Fig. 9. Tightening torque to preload relationship determined in experimental tests

The calculated values for standard properties of M6 bolts and these measured in experiments for different diameters of steel washers were collected in Table 4.

Table 4. Nut factor to bolt diameter coefficients – calculated for standard properties and experimental

Specimen type	Calculated (m)	Experimental (m)	Relative error (%)
T_12	0.00124736	0.00070890	43.2
T_18	0.00124736	0.00144820	16.1
T_24	0.00124736	0.00156250	25.3

As visible, the relative error between calculated and measured values was significant. Many factors contribute, but the primary reason is the inability to treat wood as a rigid body, leading to significant assumption changes. The solution to this problem is proposed and described in the subsequent sentences.

The basic properties of bolts as pitch of thread (p), nominal diameter (d_p), half of the thread profile angle (β) or nuts-washer as diameter of nut-bearing surface (d_n) and diameter of the bolt insert hole (d_h), should stay unchanged. Therefore, the probable reason for differences should be looked for in friction coefficients. These properties are the most uncertain and often altered by other researchers to achieve exact results [16–19]. If the bolt and nut are zinc coated and not lubricated, the friction coefficient on the thread surface (μ_s) should not change too – this can be assumed at the level of 0.15. This means that the most probable reason for differences is the change in friction coefficient on the nut bearing surface (μ_w). The explanation of this condition can be occurrence of compliant material as wood, which for a small diameter of steel washer reduces friction between nut and steel washer due to high indentation and for bigger diameters causes its increase due to bending of steel washer and nut sticking.

Thus, the author proposes agreeing of the friction coefficient on the nut bearing surface (μ_w) as a solution. To obtain proper agreement, the value of friction coefficient was gradually changed every hundredth part and the nut to bolt factors were calculated. The results of the model validation were presented in Table 5.

Table 5. Nut factor to bolt diameter coefficients – agreed for different μ_w and experimental

Specimen type	μ_w	Agreed (m)	Experimental (m)	Relative error (%)
T_12	0.02	0.00070580	0.00070890	0.4
T_18	0.20	0.00145565	0.00144820	0.5
T_24	0.23	0.00158062	0.00156250	1.2

As visible, the friction coefficient was agreed and relative error was negligible. All the determined values of friction coefficients were reliable. After agreeing the coefficients, a linear relation was found depending on the area of the nut being in contact with the steel washer ($A_n - A_h$) to the area of the washer protruding beyond the nut ($A_w - A_n$), which was presented in Fig. 10. Coefficient of function's determination was equal to ($R^2 = 0.999$).

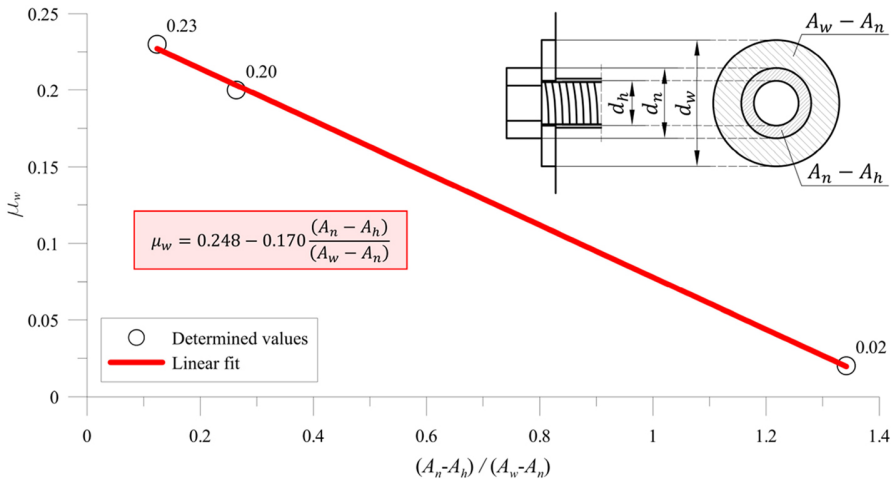

Fig. 10. Linear approximation of friction coefficient μ_w

The presented approximations can be very useful in predicting permissible tightening torque for a single bolt embedded in softwood. However, structural connections are mounted using several or dozens of bolts. Here, utilising of Finite Element Method is irreplaceable. The validated numerical model can give the value of preload force in every single bolt, which can lead to calculating proper tightening torque value using the formulas proposed earlier. Thus, crucial is to check whether the assumed method of modelling produces a proper mechanical response observed in experimental tests.

3.2. Numerical modelling

Numerical modelling included models of the same specimens as tightened in experimental tests. After the same nut factor to bolt diameter as in Table 3 was assumed to recalculate force into tightening torque value, possible was to compare results obtained from numerical simulations and to the experimental.

Direct determination of modulus of elasticity from the measurements' slopes was not possible, because the technical card of the testing machine stated that testing speed was independent of the test load acquisition. However, if the same testing speed was used in each test, the relationship between plastic to elastic modulus ($E_{pl.90}/E_{c.90}$), based on a comparison between elastic and plastic slopes of the obtained curves, was possible. The results were collected in Table 6. Relative error was less than 6%. Mean value of the modules relationship ($E_{pl.90}/E_{c.90}$) was equal to 0.4, and this was used in numerical simulations.

Table 6. Plastic to elastic modulus ($E_{pl.90}/E_{c.90}$) measurements and properties for uncertainty estimation

Specimen number	**F_12 (ϕ = 12 mm)**		**F_18 (ϕ = 18 mm)**		**F_24 (ϕ = 24 mm)**	
	$E_{pl.90}/E_{c.90}$ (·)	$(x_i-\overline{x})^2$ (·)	$E_{pl.90}/E_{c.90}$ (·)	$(x_i-\overline{x})^2$ (·)	$E_{pl.90}/E_{c.90}$ (·)	$(x_i-\overline{x})^2$ (·)
1	0.4931	0.00451	0.2947	0.00971	0.4651	0.00645
2	0.4402	0.00020	0.4740	0.00653	0.3715	0.00017
3	0.3705	0.00308	0.3677	0.00065	0.3702	0.00021
4	0.4651	0.00153	0.4057	0.00016	0.4143	0.00087
5	0.4272	0.00000	0.3731	0.00041	0.3694	0.00024
6	0.4922	0.00439	0.3674	0.00066	0.3442	0.00165
7	0.3499	0.00578	0.4926	0.00989	0.3332	0.00266
8	0.3696	0.00318	0.3702	0.00053	0.4102	0.00065
Statistical analysis	$\overline{x}$ (–)	Σ (–)	$\overline{x}$ (–)	Σ (–)	$\overline{x}$ (–)	Σ (–)
	0.4260	0.02268	0.3932	0.02853	0.3848	0.01290
	$s_{\overline{x}}$ (–)	$\frac{s_{\overline{x}}}{\overline{x}}$ (%)	$s_{\overline{x}}$ (–)	$\frac{s_{\overline{x}}}{\overline{x}}$ (%)	$s_{\overline{x}}$ (–)	$\frac{s_{\overline{x}}}{\overline{x}}$ (%)
	0.0201	4.72	0.0226	5.74	0.0152	3.94

Each simulated case met the experimental envelope of the results for the determined properties, both in elastic and plastic stage, as visible in Fig. 11. The numerical model enabled to read the value of force (F_s) in dependence on relative displacement ($2 \cdot \delta_t$). Next, the force value was recalculated into the tightening torque (T_f) based on agreed nut factor to bolt diameter coefficient ($k_f \cdot d_b$), as presented in Table 5. Despite reaching the plastic stage, the coefficient remained constant, resulting in a high accuracy of the results.

The most important part of the model is a good correlation between experimental and numerical curves. However, in case of plastic strains, possible is to compare plastic damage in the material. The phenomena observed in the numerical model comparing to the experiments were as expected, which was shown in Fig. 12.

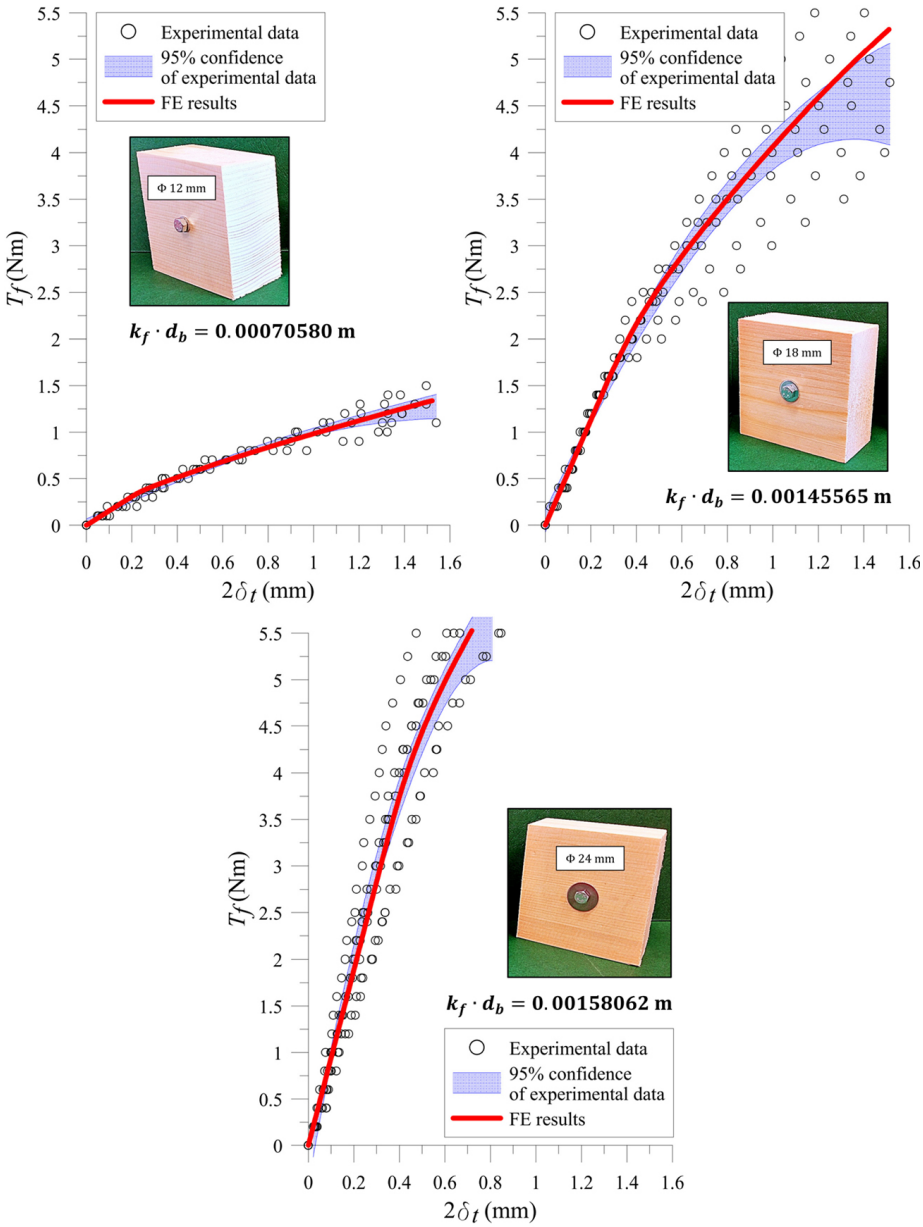

Fig. 11. Results obtained from the FE model in comparison to the experiments

The well-validated model for a single bolt can successfully predict the tightening torque-preload relationship for multiple adjacent bolts in a wooden connection, which can be the next part of the research development.

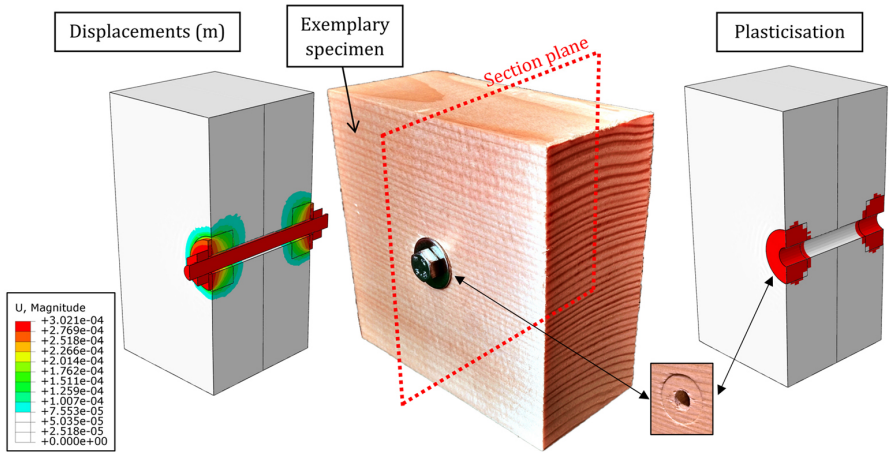

Fig. 12. Exemplary displacements field and plasticisation for $\phi 18$ specimen at $T_f = 2.8$ Nm

4. Conclusions

A basis for the research was a lack of any information on the tightening torque value for bolted connections in the timber structures' design codes. Although these connections are designed mainly on bolts' pressure on wood in parallel-to-grain direction, the statement that structural elements should be mounted "firmly" seemed to be insufficient. Due to the lack of literature, estimating the initial tightening torque or identifying the critical value that could damage the wood was challenging.

For these reasons, two experimental tests, theoretical analysis and Finite Element modelling were performed in the paper. The first experiment based on finding the tightening torque to relative displacement relationship. The next one enabled the author to check the maximal compressing force determined by theoretical approach. In this test, dependencies between plastic modulus including material's compaction and modulus of elasticity were found too and then applied to the numerical model. Tightening torque was calculated according to agreed formulas elaborated for steel structures based on the obtained preload force value. The high correlation between results from the prepared numerical models and experimental tests was observed.

The paper's assumptions have multiple applications, including but not limited to:

- Estimating a proper tightening torque value that should clamp a bolted connection. This can make easier to choose proper torque wrench to assemble bolted connection in wood without introducing too much perpendicular-to-grain plasticisation in wooden members
- Predicting stresses in connection's components and clamping pressure when connecting several elements due to tightening torque and bolt preload force introduction

At this stage of the research, the optimal value of tightening torque seems to be the one just after wood plasticisation occurs. In the author's opinion, this should guarantee a proper embedment of bolts in wooden connection using steel washers.

The author states that wider and more general engineering applications of the elaborated FE model in full-scale wooden structures can be done only after its additional validation in large-scale experiments. The research was conducted due to a lack of prior studies. Nevertheless, the paper can be a preface to more detailed investigations, which should be done in the future.

Funding

The grant was financed in the framework of the pro-quality program of Lublin University of Technology "GRANTS FOR GRANTS" (Grant no: 1/GnG/2023). Other costs were supported under Lublin University of Technology FD-20/IL-4/028 grant.

References

[1] X.T. Wang, E.C. Zhu, S. Niu, and H.J. Wang, "Analysis and test of stiffness of bolted connections in timber structures", *Construction and Building Materials*, vol. 303, art. no. 124495, 2021, doi: 10.1016/j.conbuildmat.2021.124495.

[2] N.L. Rahim, F.T.S. Sheng, A.R.A. Karim, M. Nabialek, M.M. Al Bakri Abdullah, and M. Sroka, "Effect of bolt configurations on stiffness for steel-wood-steel connection loaded parallel to grain for softwoods in Malaysia", *Archives of Civil Engineering*, vol. 68, no. 3, pp. 323–338, 2022, doi: 10.24425/ace.2022.141888.

[3] M. Johanides, D. Mikolasek, A. Lokaj, P. Mynarcik, Z. Marcalikova, and O. Sucharda, "Rotational stiffness and carrying capacity of timber frame corners with dowel type connections", *Materials*, vol. 14, no. 23, pp. 1–26, 2021, doi: 10.3390/ma14237429.

[4] M. Johanides, A. Lokaj, P. Dobes, and D. Mikolasek, "Numerical and experimental analysis of the load-carrying capacity of a timber semi-rigid dowel-type connection", *Materials*, vol. 15, no. 20, 2022, doi: 10.3390/ma15207222.

[5] C.L. dos Santos, J.J.L. Morais, and A.M.P. de Jesus, "Mechanical behaviour of wood T-joints. Experimental and numerical investigation", *Frattura ed Integrità Strutturale*, vol. 9, no. 31, pp. 23–37, 2014, doi: 10.3221/IGF-ESIS.31.03.

[6] M. Oudjene and M. Khelifa, "Elasto-plastic constitutive law for wood behaviour under compressive loadings", *Construction and Building Materials*, vol. 23, no. 11, pp. 3359–3366, 2009, doi: 10.1016/j.conbuildmat.2009.06.034.

[7] N. L. Rahim, et al., "The stiffness of steel-wood-steel connection loaded parallel to the grain", *Archives of Civil Engineering*, vol. 68, no. 2, pp. 37–50, 2022, doi: 10.24425/ace.2022.140628.

[8] PN-EN 1995-1-1:2010 Eurocode 5: Design of timber structures – Part 1-1: General-Common rules and rules for buildings. Polski Komitet Normalizacyjny, 2010.

[9] M.L. Siqueira and C.H.S. Del Menezzi, "Influence of the torque on the ultimate load of wood bolted joints", in *19th International Congress of Mechanical Engineering*. Brasilia, 2007. [Online]. Available: https://abcm.org.br/app/webroot/anais/cobem/2007/pdf/COBEM2007-0411.pdf.

[10] A. Awaludin, T. Hirai, T. Hayashikawa, Y. Sasaki, and A. Oikawa, "Effects of pretension in bolts on hysteretic responses of moment-carrying timber joints", *Journal of Wood Science*, vol. 54, no. 2, pp. 114–120, 2008, doi: 10.1007/s10086-007-0914-8.

[11] A. Awaludin, T. Hirai, T. Hayashikawa, and Y. Sasaki, "Load-carrying capacity of steel-to-timber joints with a pretensioned bolt", *Journal of Wood Science*, vol. 54, no. 5, pp. 362–368, 2008, doi: 10.1007/s10086-008-0962-8.

[12] A. Awaludin, T. Hirai, T. Hayashikawa, Y. Sasaki, and A. Oikawa, "One-year stress relaxation of timber joints assembled with pretensioned bolts", *Journal of Wood Science*, vol. 54, no. 6, pp. 456–463, 2008, doi: 10.1007/s10086-008-0985-1.

[13] A. Awaludin, T. Hirai, Y. Sasaki, T. Hayashikawa, and Oikawa, "Beam to column timber joints with pretensioned bolts", *Civil Engineering Dimension*, vol. 13, no. 2, pp. 59–64, 2011. [Online]. Available: https://ced.petra.ac.id/index.php/civ/article/view/18225/18094.

[14] S.R.F. Vieira, C.H.S. Del Menezzi, and M.L. Siqueira, "Torque and tight time effect on the ultimate load and stiffness of maçaranduba (*Manikara huberi* Ducke A. Chev) wood bolted joint", *Scientia Forestalis*, vol. 37, no. 84, pp. 459–464, 2009. [Online]. Available: https://www.ipef.br/publicacoes/scientia/nr84/cap13.pdf.

[15] D. Matsubara, Y. Wakashima, H. Shimizu, and A. Kitamori, "The load factor in bolted timber joints under external tensile loads", *Journal of Wood Science*, vol. 66, no. 1, 2020, doi: 10.1186/s10086-020-01857-4.

[16] S. Izumi, T. Yokoyama, A. Iwasaki, and S. Sakai, "Three-dimensional finite element analysis of tightening and loosening mechanism of threaded fastener", *Engineering Failure Analysis*, vol. 12, no. 4, pp. 604–615, 2005, doi: 10.1016/j.engfailanal.2004.09.009.

[17] Q. Yu, H. Zhou, and L. Wang, "Finite element analysis of relationship between tightening torque and initial load of bolted connections", *Advances in Mechanical Engineering*, vol. 7, no. 5, pp. 1–8, 2015, doi: 10.1177/1687814015588477.

[18] Q.M. Yu, X.J. Yang, and H.L. Zhou, "An experimental study on the relationship between torque and preload of threaded connections", *Advances in Mechanical Engineering*, vol. 10, no. 8, 2018, doi: 10.1177/1687814018797033.

[19] H. Gong, J. Liu, and X. Ding, "Calculation of the effective bearing contact radius for precision tightening of bolted joints", *Advances in Mechanical Engineering*, vol. 8, no. 9, pp. 1–8, 2016, doi: 10.1177/1687814016668445.

[20] R.J. Ross, C.D. Risbrudt, M.A. Ritter, and T.H. Wegner, *Wood Handbook: Wood as an Engineering Material*. Madison, Wisconsin: United States Department of Agriculture Forest Service, Forests Products Laboratory, 2010, doi: 10.2737/FPL-GTR-190.

[21] A.J.M. Leijten, A.J.M. Jorissen, and B.J.C. De Leijer, "The local bearing capacity perpendicular to grain of structural timber elements", *Construction and Building Materials*, vol. 27, no. 1, pp. 54–59, 2012, doi: 10.1016/j.conbuildmat.2011.07.022.

[22] A.J.M. Leijten, H.J. Larsen, and T.A.C.M. Van der Put, "Structural design for compression strength perpendicular to the grain of timber beams", *Construction and Building Materials*, vol. 24, no. 3, pp. 252–257, 2010, doi: 10.1016/j.conbuildmat.2009.08.042.

[23] T.A.C.M. Van Der Put, "Derivation of the bearing strength perpendicular to the grain of locally loaded timber blocks", *Holz als Roh – und Werkstoff*, vol. 66, no. 6, pp. 409–417, 2008, doi: 10.1007/s00107-008-0258-0.

[24] R.H. Hemanth, et al., "Performance evaluation of finite elements for analysis of advanced hybrid laminates", in *ABAQUS User's Conference*. 2010, pp. 1–15.

Metoda przewidywania momentu dokręcania i siły sprężającej dla śrub osadzonych w drewnie iglastym przy użyciu podkładek stalowych

Słowa kluczowe: przewidywanie siły sprężającej i momentu dokręcenia, śruby osadzone w drewnie miękkim, badania eksperymentalne, modelowanie metodą Elementów Skończonych

Streszczenie:

W artykule przedstawiono badania dotyczące przewidywania momentu dokręcenia i siły sprężającej dla śrub osadzonych w miękkim drewnie iglastym przy użyciu podkładek stalowych. Podstawą badań był brak informacji o wartości momentu dokręcenia śrub w połączeniach śrubowych w normach projektowych konstrukcji drewnianych. Z tego powodu w artykule przeprowadzono dwa badania eksperymentalne, analizę teoretyczną oraz modelowanie Metodą Elementów Skończonych. Pierwsze doświadczenie polegało na wyznaczeniu zależności momentu dokręcenia od przemieszczenia względnego. Kolejne umożliwiło autorowi sprawdzenie maksymalnej siły ściskającej określonej teoretycznie. W teście tym znaleziono także zależności pomiędzy modułem plastycznym uwzględniającym zagęszczeniem materiału i modułem sprężystości, które następnie zastosowano do modelu numerycznego. Moment dokręcenia obliczono na podstawie ustalonych wzorów opracowanych dla konstrukcji stalowych bazując na uzyskanej

wartości siły sprężającej. Zaobserwowano wysoką korelację pomiędzy wynikami opracowanych modeli numerycznych i wynikami badań eksperymentalnych. Badania przedstawione w artykule mają wiele zastosowań, jak oszacowanie właściwej wartości momentu dokręcenia, jaki powinien zostać wprowadzony do połączenia śrubowego, przewidywanie naprężeń w elementach połączenia i docisku podczas łączenia kilku elementów na skutek wprowadzenia momentu dokręcenia i siły sprężającej śruby, czy przewidywanie reakcji konstrukcji połączeń na wiele śrub w pierwszej fazie obciążenia.

Received: 2023-12-12, Revised: 2024-02-06